Investigation of plasma turbulence in strongly sheared $E \times B$ flows using multi-probe arrays

M. RAMISCH[1)], F. GREINER[2)], N. MAHDIZADEH[1)], K. RAHBARNIA[1)] and U. STROTH[1)]

[1)]*Institut für Plasmaforschung, University Stuttgart, 70569 Stuttgart, Germany*
[2)]*Institut für Experimentelle und Angewandte Physik, University Kiel, 24098 Kiel, Germany*

Poloidal $E \times B$ shear flows can act on turbulent transport through the shear decorrelation mechanism, which can reduce the radial size of turbulent structures [1] or change the phase relation between density and potential fluctuations [2]. In this contribution, the influence of sheared $E \times B$ flows on the microscopic structure of turbulence is investigated in the toroidally confined plasma of the torsatron TJ-K. Multi-probe arrays are used to detect turbulent structures and study the dynamics perpendicular to the magnetic field. Sheared poloidal $E \times B$ flows are generated by plasma biasing. It turns out that at strong flow shear, the fluctuations are dominated by large-scale coherent structures with increased correlation and poloidal wave lengths. Constant particle flux is realised at steeper gradients due to modifications of the cross-phase, which relates the large-scale structures to inward transport.

Keywords: drift-wave turbulence, shear flows, turbulence suppression, biasing, probe array, torsatron TJ-K.

1 Introduction

The understanding of the formation of transport barriers during transitions from low-confinement (L-mode) to high-confinement (H-mode) regimes is one of the key objectives in fusion research. Poloidal $E \times B$ shear flows are widely accepted as a trigger mechanism of transport barriers in the edge of fusion plasmas [3]. This has been confirmed in experiments with spontaneously excited transport barriers [2] and such triggered by external plasma biasing [4]. Strong $E \times B$ flows can act on turbulent transport through the shear decorrelation mechanism [1], which can reduce the radial size of turbulent structures or change the phase relation between density and potential fluctuations [2].

For interchange and ion-temperature-gradient driven turbulence it was found that a transport reduction by sheared flows is mostly due to a reduction of the fluctuation amplitudes [5]. Other analytical studies suggested, however, that strong shear flows predominantly influence the cross-phase leading to reduced or in case of collisional drift-waves even locally inward directed transport [6]. In fact, strong cross-phase modifications have already been observed during spontaneous [7] as well as externally induced L-H transitions [8].

In this work, the influence of strong $E \times B$ shear flows on the microscopic structure of turbulence is investigated in high detail using multi-probe arrays inside the confinement region of a toroidal plasma. The experiments are carried out on the low-temperature plasma of the torsatron TJ-K, which is dimensionally similar to fusion edge plasmas [9]. $E \times B$ flows are generated by biasing an internal flux surface.

author's e-mail: ramisch@ipf.uni-stuttgart.de

2 Experimental setup

The torsatron TJ-K [10] toroidally confines a low-temperature plasma, which is dimensionally similar to fusion edge plasmas [9]. The major and the minor plasma radius is $R_0 = 0.6\,\mathrm{m}$ and $a = 0.1\,\mathrm{m}$, respectively. The confining magnetic field has a rotational transform of about $1/3$ with low magnetic shear. TJ-K can be operated with nominal magnetic field strengths in the range $B = 70$–$100\,\mathrm{mT}$ when electron-cyclotron-resonance heating (ECRH) at 2.45 GHz is used for plasma generation. In the present experiment, the working gas was hydrogen at a neutral gas pressure of $p_0 = 4 \times 10^{-5}\,\mathrm{mbar}$, a heating power of $P_{\mathrm{ECRH}} = 1.8\,\mathrm{kW}$ and a magnetic field strength of $B = 72\,\mathrm{mT}$. For these parameters, the typical electron temperature and maximum density is $T_e \approx 7\,\mathrm{eV}$ and $n \approx 2 \times 10^{17}\,\mathrm{m}^{-3}$, respectively. The ions are cold ($T_i < 1\,\mathrm{eV}$).

In order to generate the appropriate $E \times B$ flow, an electrode consisting of a closed stainless steel wire in the shape of the poloidal cross-section of an inner flux surface was used. The wire had a diameter of 3 mm. It was biased positively with respect to the grounded vacuum vessel via a single lead, which was insulated by a ceramics tube. A grounded electrode will be referred to as unbiased. The electrode was introduced from a top port at a toroidal angle of $\phi = 50°$, where the flux surfaces are elliptical. Equilibrium-profile and fluctuation measurements have been carried out at two outer ports at $\phi = 270°$ or $330°$ and $\phi = 90°$, respectively. At the positions of the outer ports, the flux-surface cross-sections are triangular. In Fig. 1, the mapping of the electrode onto such a position is shown.

For the measurements of turbulent structures in the density fluctuations, two diagnostics consisting of 64

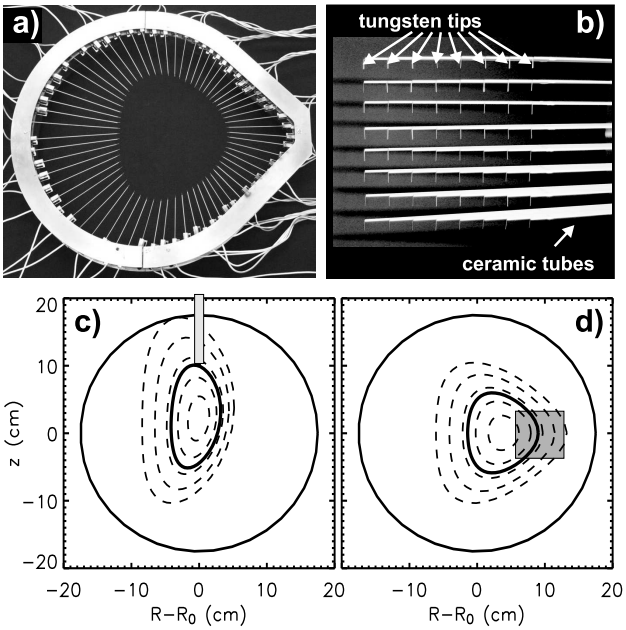

Fig. 1 Photo of the poloidal 64-tip probe array (a) and the 8×8 probe matrix (b). Position of the electrode inside the separatrix (c) and mapping onto the probe section (d). The shaded area depicts the region covered by the probe matrix.

Langmuir probes were used. The first diagnostics is set up on a two-dimensional grid of 8×8 points in the poloidal cross-section on the low-field side and centered at the biased surface as shown in Fig. 1. The spatial resolution is 1 cm in vertical and horizontal direction. At all 64 positions, the fluctuations in the ion-saturation current were simultaneously acquired with 16 bit accuracy at a rate of 1 MHz within a time interval of 1 s. Cross-correlation analyses carried out on these data reveal the spatio-temporal evolution of turbulent density structures. The cross-correlation between each probe of the matrix at a position (R_i, z_j) and one reference probe as a function of a time lag Δt is calculated according to

$$C_{i,j}(\Delta t) = \int \frac{\widetilde{n}_{\mathrm{ref}}(t)}{\sigma_{\mathrm{ref}}} \frac{\widetilde{n}_{i,j}(t+\Delta t)}{\sigma_{i,j}} \, \mathrm{d}t, \qquad (1)$$

where each signal is normalised to its respective rms value σ. In Ref. [11], the probe array and the analysis technique is introduced in more detail. In order to resolve the poloidal structure of turbulence, the matrix has been replaced by a poloidal probe array. The probes are poloidally arranged on a complete circumference of a flux surface near the biased one with a poloidal resolution of 7 mm. Both the poloidal and the two-dimensional probe array are shown in Fig. 1.

3 Perpendicular dynamics without strong $E \times B$ flow

In TJ-K, the turbulence drive is governed by drift waves. Evidence for drift-wave signatures in the spectral cross-phase between density and potential fluctuations and for the parallel structure in toroidal geometry is provided in Ref. [9] and [12], respectively.

In order to investigate the dynamics perpendicular to the magnetic field, turbulent structures are used as tracers of the background flow. Therefor, cross-correlation analyses according to Eq. (1) are carried out on density fluctuations measured with the matrix. For consecutive time lags Δt, the result is shown in Fig. 2. Quasi-coherent structures

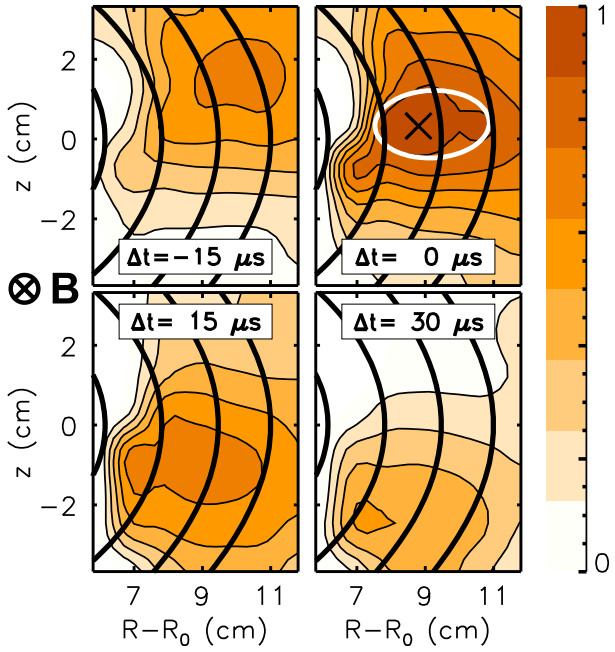

Fig. 2 Contour plots of cross-correlations between matrix probes with the reference probe located at (×). The ellipse at $\Delta t = 0$ approximates the structure size at 87 % correlation.

are observed, which propagate clockwise with a speed of about 800 ms^{-1}. The direction corresponds to the direction of the electron-diamagnetic drift U_{dia}. Since the radial electric field is weak, the poloidal $E \times B$ flow velocity is negligible compared to U_{dia}. Hence, the propagation is in agreement with expectations from the linear drift-wave dispersion relation [13]

$$\omega \approx U_{\mathrm{dia}} k_\perp / (1 + k_\perp^2 \rho_s^2), \qquad (2)$$

where $k_\perp$ is the perpendicular wavenumber and $\rho_s = \sqrt{T_e M_i}/eB$ the drift-scale with T_e the electron temperature, M_i the ion mass and B the magnetic field strength. For the discharge presented in Fig. 2, the normalised wavenumber $k_\perp \rho_s$ is about 0.26 [14]. Therefore, the propagation velocity directly reflects the electron-diamagnetic drift velocity

within a deviation of 6 %. In Fig. 2, the approximate structure size at 87 % correlation at $\Delta t = 0$ is indicated by an ellipse and will be used below for comparison with the case, where strong flow shear is present.

4 Influence of shear flows on the perpendicular dynamics

In order to generate a strong $E \times B$ shear flow, the electrode was biased to 100 V. In Fig. 3, the effect on the potential profile is shown. The potential inside the biased surface is

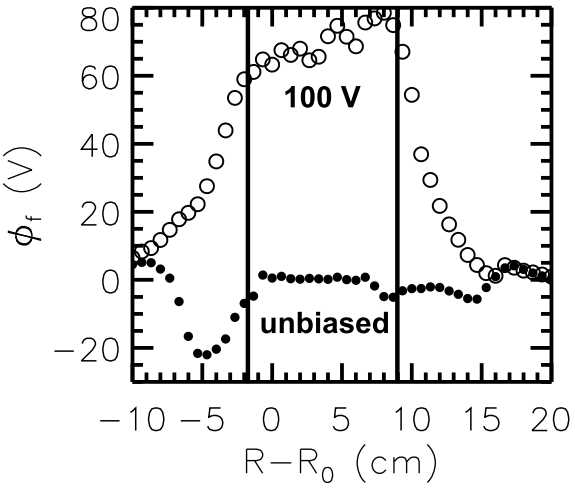

Fig. 3 Radial profile of the floating potential for the unbiased (•) and the biased case (○). Vertical lines mark the position of the biased flux surface.

strongly increased leading to enhanced radial electric fields outside. The potential drops by about 80 V over a distance of 7 cm. The resulting radial electric field of 1100 Vm^{-1} corresponds to a poloidal $E \times B$ velocity of $U_{E\times B} = 16$ kms^{-1}. The shearing rate of the generated flow with values between 100 and 400 kHz in almost the entire radial range becomes larger than the decorrelation rate of about 50 kHz in the unbiased case. At the same time, the density gradient is steepened by a factor of five [15].

In the biased state, turbulent structures have been measured with the probe matrix and detected by cross-correlation analyses. The result is shown in Fig. 4. In comparison with the unbiased state (see Fig. 2), the propagation points into the opposite direction, i.e., in the direction of the $E \times B$ drift. The propagation speed is increased by a factor of 15 from 0.8 to about 12 kms^{-1}. This can be understood directly by taking into account the changes in the equilibrium profiles. For the unbiased case, the potential profile in Fig. 3 does not show steep gradients, which would lead to substantial radial electric fields and, thus, poloidal $E \times B$ rotation. The propagation of the structures is governed by the electron-diamagnetic drift velocity. During biasing, the density gradient and, therefore, U_{dia} increased by a factor of five to 4 kms^{-1} ($k_\perp \rho_s$ reduces

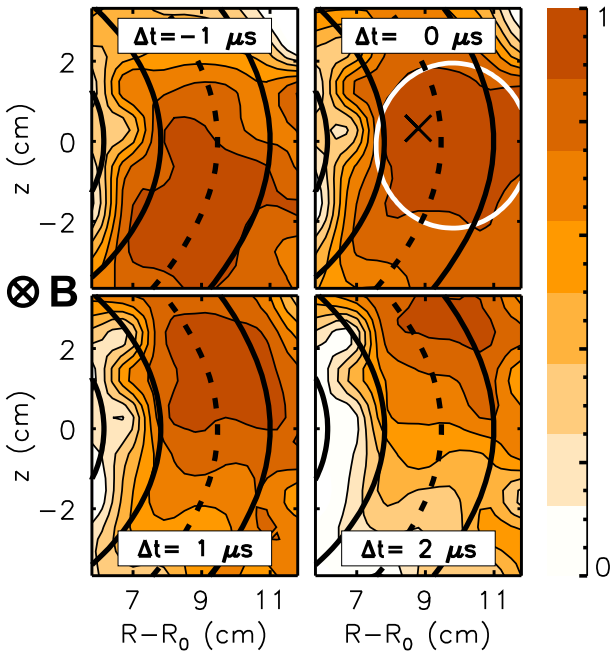

Fig. 4 Contour plots of cross-correlations between matrix probes with the reference probe in the same representation as in Fig. 2 (but note the different time windows in both cases). Here, the dashed line marks the biased flux surface.

to 0.2, see below). But now, $U_{E\times B} = 16\,\mathrm{kms}^{-1}$ dominates the poloidal flow resulting in a poloidal propagation speed of 12 kms^{-1}.

Strong flow shear as in the biased case with shearing rates larger than the turbulence decorrelation rate in the absence of shear is expected to reduce the radial correlation length of turbulent structures [1]. However, instead of a reduction an increase in the structure size is observed, when figures 2 and 4 are compared. The structure becomes more circular and essentially exceeds the matrix dimensions.

5 Poloidal mode structure under strong shear

For a proper statement on the change in the mode structure, the comparative biasing studies have been repeated with the poloidal probe array. Density fluctuations have been recorded under the same conditions and cross-correlation analyses have been carried out on the data. The mode structure as a function of the poloidal coordinate Δs with respect to the reference probe is represented by the cross-correlation function at $\Delta t = 0$. The calculation was done with all 64 probes one by one taken as reference probe. Then the 64 correlation functions have been averaged. For the unbiased and biased case, the result is shown in Fig. 5. It can be seen that the poloidal mode structure changes from $m = 4$ to $m = 3$ during biasing. With a safety factor of about $q \approx 3$, this corresponds to a single helical

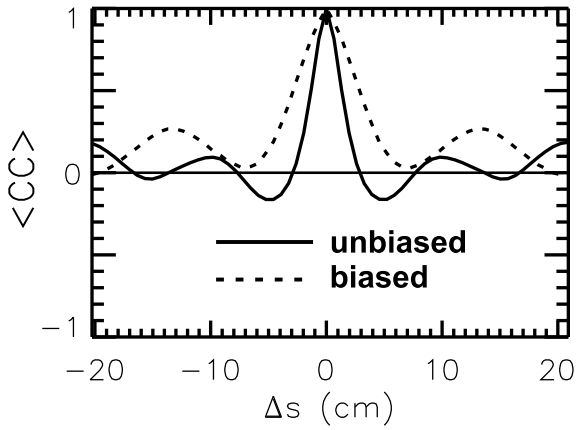

Fig. 5 Average spatial poloidal mode structure in the unbiased (solid) and the biased case (dashed line). The mode structure changes from $m = 4$ to $m = 3$ during biasing.

structure.

During biasing, the local value of ρ_s at the centre position of the structure stays constant, while the poloidal wavelength increases by a factor of 4/3, which reduces $k_\perp \rho_s$ from 0.26 to about 0.2. Hence, the contribution of the diamagnetic drift to the total propagation velocity of the large-scale structure is still consistent with the linear dispersion relation of drift waves given by Eq. (2).

In the unbiased case, $m = 3$ with $U_{\mathrm{dia}} = 800\,\mathrm{ms}^{-1}$ corresponds to a frequency of about 5 kHz. An increase of the poloidal rotation by a factor of 15 would lead to a shift of this mode to about 75 kHz. In fact, the large-scale structure is related to a dominant peak at 72 kHz in the power spectrum. Modes $m \geq 4$ were found to be suppressed. The $m = 3$ mode was shown to be related to local turbulent inward transport due to a modification of the cross-phase between density and potential fluctuations [15]. The total particle flux, thus, remains unchanged compared to the unbiased case, i.e., the same flux is realised at steeper density gradients, which implies an improvement of the particle confinement.

In H-mode fusion plasmas, reduced radial correlation lengths were found in the shear layer [16]. However, the results presented here rather point to the importance of the phase relation between density and potential fluctuations for confinement improvement. Significant cross-phase modifications have been predicted for systems with a quasi-coherent fluctuation spectrum [6] under the influence of very strong shear like in the present case and such modifications have also been found during H-mode discharges in several devices (see, e.g., Refs. [7, 8, 17]).

6 Summary

The influence of strong $E \times B$ shear flows on the microscopic structure of drift-wave turbulence has been investigated by means of multi-probe arrays. Turbulent density structures were detected with an 8×8-probe array perpendicular to the magnetic field inside the confinement region of the torsatron TJ-K. The poloidal mode structure was measured with a 64-tip poloidal probe array. The $E \times B$ flow was generated by biasing an internal flux surface. This way, a poloidal $E \times B$ flow with a velocity of about $16\,\mathrm{kms}^{-1}$ and a shearing rate larger than 100 kHz with a maximum value of about 400 kHz has been achieved. At the same time, the density gradient steepened by a factor of 5. In both the unbiased and biased case, the propagation of turbulent structures, which were used as tracers of the background flow, was due to poloidal $E \times B$ and electron-diamagnetic drift velocities in agreement with the linear drift-wave dispersion relation. During biasing, the turbulence suppression criterion [1] was well fulfilled in almost the entire radial range. However, the fluctuations were found to be dominated by large-scale structures. The characteristic poloidal mode structure changed from $m = 4$ to $m = 3$. Hence, it has been demonstrated that strong shear can change the spatial structure of drift-wave turbulence in toroidal geometry in favour of coherent structures with larger correlation lengths. In Ref. [15], these structures were shown to be associated with local turbulent inward transport due to modifications in the phase relation between density and potential fluctuations.

References

[1] H. Biglari, P. H. Diamond, and P. W. Terry, Phys. Fluids, B **2**, 1 (1990).
[2] K. H. Burrell, Phys. Plasmas **4**, 1499 (1997).
[3] K. Itoh and I. Sanae-I, Plasma Phys. Controll. Fusion **38**, 1 (1996).
[4] R. J. Taylor *et al.*, Phys. Rev. Lett. **63**, 2365 (1989).
[5] E.-J. Kim, P. H. Diamond, and T. S. Hahm, Phys. Plasmas **11**, 4554 (2004).
[6] P. W. Terry, D. E. Newman, and A. S. Ware, Phys. Plasmas **10**, 1066 (2003).
[7] R. A. Moyer *et al.*, Phys. Plasmas **2**, 2397 (1995).
[8] J. A. Boedo *et al.*, Phys. Rev. Lett. **84**, 2630 (2000).
[9] U. Stroth *et al.*, Phys. Plasmas **11**, 2558 (2004).
[10] N. Krause *et al.*, Rev. Sci. Instrum. **73**, 3474 (2002).
[11] M. Ramisch *et al.*, Phys. Plasmas **12**, 032504 (2005).
[12] N. Mahdizadeh *et al.*, Plasma Phys. Controll. Fusion **49**, 1005 (2007).
[13] M. Wakatani and A. Hasegawa, Phys. Fluids **27**, 611 (1984).
[14] M. Ramisch, E. Häberle, N. Mahdizadeh, and U. Stroth, submitted to Plasma Sources Sci. Technol. (2007).
[15] M. Ramisch *et al.*, Plasma Phys. Controll. Fusion **49**, 777 (2007).
[16] J. Schirmer *et al.*, Plasma Phys. Controll. Fusion **49**, 1019 (2007).
[17] M. G. Shats *et al.*, Phys. Rev. Lett. **84**, 6042 (2000).